JOURNAL OF GEOPHYSICAL RESEARCH, VOL. 95, NO. B12, PAGES 19,311–19,325, NOVEMBER 10, 1990

Fundamental Thermodynamic Relations and Silicate Melting With Implications for the Constitution of D''

LARS STIXRUDE AND M. S. T. BUKOWINSKI

Department of Geology and Geophysics, University of California, Berkeley

We describe fundamental thermodynamic relations (Helmholtz free energy as a function of volume and temperature) for solids and liquids, simple physically based expressions which contain all thermodynamic information about a system. The solid fundamental relation consists of Debye and Birch-Murnaghan finite-strain theory combined in the Mie-Grüneisen framework. The liquid fundamental relation is derived by taking the high-temperature limit of the solid expression. We derive the liquid equation of state, which contains only four parameters, from the liquid fundamental relation and show that it successfully describes measurements of liquid alkali metals, water, and liquid diopside over a wide range of pressure and temperature. We find optimal fundamental relation parameters for diopside, enstatite, ilmenite, and perovskite and find the solid relation to be in excellent agreement with data, including heat capacities, thermal expansion, and $MgSiO_3$ phase equilibria. We then combine the liquid and solid fundamental relations to calculate the melting curves of diopside, enstatite, and perovskite, which are found to be in excellent agreement with experiment. All predicted melting curves have dT/dP slopes which decrease steadily with pressure, eventually becoming negative because of liquid-crystal density inversion. Our predicted melting temperature of perovskite in the D'' region (3750 K) at the base of the mantle is thousands of degrees lower than previous estimates, yet it is consistent with experimental data. The predicted melting curve, although consistent with the lack of widespread melting in the lower mantle, is much lower than recently proposed geotherms in the D'' layer at the base of the mantle. By combining our results with seismic observations of the deep mantle, we propose that the D'' layer consists of magnesiowüstite and silica in the form of stishovite or its recently discovered high-pressure modification.

INTRODUCTION

Melting is one of the most important agents of chemical and thermal planetary evolution. The production and subsequent transport of mobile liquids lead to efficient mass and heat transport in planetary interiors. It has loon been thought that all less basic Earth material is ultimately derived, via incongruent melting processes, from ultrabasic material, taken as representative of the Earth's bulk chemistry [*Bowen*, 1928, chapter 17]. Subsequent geologic and geochemical evidence has confirmed that igneous processes are primarily responsible for the origin and evolution of the acidic continental crust [*Fyfe*, 1978; *Depaolo*, 1981] and for the ongoing formation of the basaltic oceanic crust [*Hess*, 1962].

More recently, the possibility that larger fractions of the silicate Earth have undergone chemical differentiation by igneous processes has been examined in detail [*Stolper et al.*, 1981; *Nisbet and Walker*, 1982]. Indeed, there seems to be no shortage of energy sources sufficient to melt the entire Earth early in its history, including accretion [*Hanks and Anderson*, 1969], core formation [*Flasar and Birch*, 1973; *Sasaki and Nakazawa*, 1986], and giant impacts [*Stevenson*, 1987]. Thus several models for the separation of partial melt from residual crystals in mantle-sized magma chambers have been advanced [*Ohtani*, 1983, 1988; *Herzberg*, 1984; *Anderson and Bass*, 1986] which help to explain recent evidence that the lower mantle, and perhaps the transition zone as well, may be chemically distinct from the upper mantle.

Thermal, as well as chemical, evolution is greatly affected by melting: the advective transport of heat resulting from partial melting at mid-ocean ridges accounts for most of the heat lost from the Earth [*Sclater et al.*, 1981]. Finally, through knowledge of silicate solidi, the observation that the present mantle contains at most a few percent partial melt places constraints on the Earth's temperature distribution. Thus knowledge of silicate melting curves is of fundamental importance in determining the present state of the Earth's interior and in constructing theories of terrestrial chemical and thermal evolution.

Despite its importance, little is known about the melting of silicates throughout most of the Earth's pressure regime. While high-pressure experimental data have begun to appear only recently, attempts to predict high-pressure melting behavior of Earth materials have a long history in geophysics [*Uffen*, 1952; *Higgins and Kennedy*, 1971; *Stacey and Irvine*, 1977; *Boschi et al.*, 1979; *Ohtani*, 1983; *Simon*, 1953; *Mulargia and Quareni*, 1988; *Poirier*, 1989]. Most have relied on variants of the Lindemann [*Lindemann*, 1910] theory of melting or related empirical forms such as the Kraut-Kennedy [*Kraut and Kennedy*, 1966] and *Simon* [*Simon*, 1953] equations (for a derivation of these three approaches from a generalized Lindemann Law, see *Ross* [1969]). The Lindemann Law successfully describes the melting of simple close-packed substances such as rare gases [*Ross*, 1969; *Wolf and Jeanloz*, 1984]. However, although the simplicity of these methods is appealing, the underlying physical assumptions of Lindemann-type models are not justified for the complex silicate structures of interest here [*Stacey and Irvine*, 1977], and they are unable to reproduce observed silicate melting curves even at low pressures [*Wolf and Jeanloz*, 1984]. Therefore existing theories of melting cannot be used to reliably predict silicate melting in the deep Earth.

Instead of melting theories, several authors have taken a thermodynamic approach: constructing models for the free energy of the liquid and solid phases which must be equal

Paper number 90JB01680.
0148-0227/90/90JB-01680$05.00

along the melting curve [*Bottinga*, 1985; *Lange and Carmichael*, 1987; *Rigden et al.*, 1989; *Fei et al.*, 1990]. However, these studies were limited to relatively low pressure ($P < 20$ GPa), and the application of this approach to higher pressures has suffered from the lack of a generally successful functional form of the liquid free energy, upon which the calculation critically depends. Although successful forms exist for the solid [*Knopoff*, 1963], liquid models are generally restricted to matching data over a limited range of pressure and temperature and have not been extensively tested under deep mantle conditions. Thus the form of the liquid free energy represents a major uncertainty in using this method to predict high-pressure silicate melting.

Here we construct general physically based fundamental thermodynamic relations for solids and liquids that allow us to reliably predict silicate melting curves throughout the pressure regime of the Earth's mantle. The fundamental relations, which contain complete thermodynamic information, including equations of state and phase equilibria, combine Birch-Murnaghan finite-strain theory and the Debye theory of thermal energy within the Mie-Grüneisen framework. We review a simple parametric expression for the solid fundamental relation, and by taking its high-temperature limit, the corresponding expression for liquids is derived. We then show that the liquid fundamental relation is in excellent agreement with pressure-temperature equation of state data for a variety of liquids, including the alkali metals, water, and liquid diopside. After describing in detail a procedure for obtaining optimal values of solid silicate model parameters, we combine the solid and liquid fundamental relations to calculate the melting curves of enstatite, diopside, and perovskite, which are in excellent agreement with experiment. Finally, we discuss the geophysical implications of the predicted perovskite melting temperature at the base of the mantle.

Fundamental Thermodynamic Relations and Equations of State

Following *Callen* [1985, p. 28], we use the term "fundamental thermodynamic relation" to describe any relation between thermodynamic variables which contains all thermodynamic information about a system. Examples include the Gibb's free energy as a function of temperature and pressure; entropy as a function of internal energy and volume; and the type of interest here, the Helmholtz free energy as a function of volume and temperature [*Callen*, 1985, chapter 5]. "Fundamental" does not imply that in actual applications the method is based on first principles. In practice it is necessary to find approximate expressions for the thermodynamic potentials, and the parameters in these expressions may be constrained by theory, data, and/or systematics.

The framework for a fundamental thermodynamic relation of solids was pioneered by *Mie* [1903] and *Grüneisen* [1912], whose theory explained temperature dependent phenomena at low pressure very successfully. However, they lacked the remarkably accurate finite-strain theory, refined later by *Birch* [1952], to describe the behavior of solids at high pressure. The Birch-Murnaghan equation of state has subsequently found wide application in determining the nature of the Earth's interior. While the equation of state has proved extremely useful to geophysics, a return to the more general fundamental relation formalism is important since it allows, in addition to the equation of state, complete information about the complex high-pressure phase equilibria in the Earth (see, for example, *Liu and Bassett* [1986]) and melting, the primary concern of this paper.

Our goal is to construct a simple, physically based, parametric model which gives the Helmholtz free energy F as a function of volume V and temperature T and which thus contains all thermodynamic information about the model system [*Callen*, 1985]. Following *Grüneisen* [1912], we begin by assuming that F can be divided into a "cold" part, F_c, which depends only on volume, and a thermal part, F_{TH}:

$$F(V, T) = F_0 + F_c(V, T_0) + \{F_{TH}(V, T) - F_{TH}(V, T_0)\} \quad (1)$$

where subscript 0 indicates reference values at zero pressure and T_0. We assume that F_c is represented by the Birch-Murnaghan finite-strain theory [*Birch*, 1952, 1978] which has been extensively tested against high-pressure data and is thus known empirically to give an excellent account of the compression of both solids and liquids [see *Jeanloz*, 1988, and references therein; *Jeanloz*, 1989]:

$$F_c = 9K_0V_0[\tfrac{1}{2}f^2 + \tfrac{1}{3}a_1f^3 + \tfrac{1}{4}a_2f^4 + \cdots] \quad (2a)$$

$$f = \tfrac{1}{2}[(V_0/V)^{2/3} - 1] \quad (2b)$$

$$a_1 = \tfrac{3}{2}(K_0' - 4) \quad (2c)$$

$$a_2 = \tfrac{3}{2}[K_0K_0'' + K_0'(K_0' - 7) + 143/9] \quad (2d)$$

where K is the bulk modulus and K' and K'' are its first and second pressure derivatives, respectively. Unless otherwise noted, the series in (2a) will be truncated after the f^3 term, yielding the third-order Birch-Murnaghan form.

Within the quasi-harmonic approximation [*Born and Huang*, 1954, section 4], F_{TH} is characterized by an integral over the vibrational density of states $g(w)$ of the crystal:

$$F_{TH} = kT\int_0^\infty \ln\,(1 - e^{-t})g(t)\,dt \quad (3)$$

where k is Boltzmann's constant. We neglect anharmonic terms, to first order proportional to T^2 [*Wallace*, 1972], since these are found experimentally to be very small [*Anderson et al.*, 1982] and, for the materials considered here, unresolvable; (3) is an excellent description of the data (see below). Although the data do not constrain the role of anharmonicity outside the experimental range of pressure and temperature, theoretical results indicate that anharmonicity is probably unimportant throughout the Earth's pressure-temperature regime [*Hardy*, 1980]. For typical silicate debye temperatures and bulk moduli, anharmonic corrections to the pressure are found to be less than 5% at typical melting points in the limit of zero pressure and to decrease rapidly with increasing pressure, to less than 1% at D'' PT conditions [*Hardy*, 1980].

It will be sufficient here to represent $g(w)$ by a single characteristic frequency w_0 (related to a characteristic temperature by $\theta_0 = hw_0/k$, where h is Planck's constant). Although more complex forms can be derived [e.g., *Kieffer*, 1979; *Chopelas*, 1990], thermodynamics at all but very low

temperatures ($T/\theta < 0.1$, well below temperatures of interest here) are virtually insensitive to the detailed form of the density of states. This accounts for the success of one-parameter models of $g(w)$, due to *Einstein* [1907] and *Debye* [1912], which approximate the density of states with a root-mean-square frequency (θ_{0E}) and a maximum cutoff frequency (θ_{0D}), respectively (see also *Born and Huang* [1954, p. 44]). We compare the predictions of these two models throughout and confirm that they are virtually indistinguishable except at very low temperatures (well below room temperature), emphasizing the insensitivity of thermodynamics to approximations of the density of states (see also *Born and Huang* [1954, p. 44]).

In the Debye model, F_{TH} is given by

$$F_{TH}(V, T) = 9nRT(T/\theta)^3 \int_0^{\theta/T} \ln (1 - e^{-t}) t^2 \, dt \quad (4)$$

and in the Einstein model by

$$F_{TH}(V, T) = 3nRT \ln (1 - e^{-\theta/T}) \quad (5)$$

where n is the number of atoms in the formula unit, R is the gas constant, and θ is the characteristic temperature. Although zero point vibrational terms must be included when comparing theoretical static calculations to data (see, for example, *Stixrude and Bukowinski* [1988]), they are implicitly included in $F_c(V, T_0)$ for any observable T_0 and thus do not appear in (3). For simplicity, explicit expressions for thermodynamic properties, which merely involve derivatives of the fundamental relation, will be given only for the Debye model.

Following *Grüneisen* [1926] we assume that the characteristic temperature θ depends only on volume. This dependence is described by the Grüneisen parameter (see also *Born and Huang* [1954, pp. 48–49] and *Knopoff* [1963]),

$$\gamma \equiv -d \ln \theta / d \ln V \quad (6a)$$

whose volume dependence is assumed to be

$$\gamma = \gamma_0 (V/V_0)^q \quad (6b)$$

so that

$$\theta = \theta_0 \exp [(\gamma_0 - \gamma)/q] \quad (6c)$$

The logarithmic volume derivative of γ, q, is assumed to be 1 ± 1 throughout, a good approximation for a wide variety of materials [*Anderson*, 1974; *Boehler and Ramakrishnan*, 1980; *Boehler*, 1982].

Equations (1)–(6) give the form of the fundamental relation for solids. A large body of data has shown that this fundamental relation, most often seen in the form of the Mie-Grüneisen equation of state,

$$\begin{aligned} P(V, T) &= -(dF/dV)_T \\ &= P_c(V, T_0) + [P_{TH}(V, T) - P_{TH}(V, T_0)] \\ &= 3K_0 f(1 + 2f)^{5/2}[1 + a_1 f + a_2 f^2 + \cdots] \\ &\quad + \gamma/V[E_{TH}(V, T) - E_{TH}(V, T_0)] \end{aligned} \quad (7)$$

where the Debye thermal energy is

$$E_{TH} = 9nRT(T/\theta)^3 \int_0^{\theta/T} t^3/(e^t - 1) \, dt \quad (8)$$

is accurate [*Shapiro and Knopoff*, 1969; *Knopoff and Shapiro*, 1969; *Jeanloz*, 1989]. However, less data are available for liquids, and the proper form of a liquid fundamental relation is less certain. Therefore in order to find the simplest possible expression which is consistent with the data, we derive a simplified version of the solid fundamental relation to represent liquids.

Much of the complexity of (1)–(6) results from the importance of quantum effects in solids at low temperatures ($T < \theta$). Since liquids are inherently high temperature phenomena (silicate melting temperatures are typically 2–3 times larger than θ), we consider the high-temperature limit of (1)–(6). To first order in θ/T we have

$$F_{TH} = 3nRT[\ln (\theta/T) - \tfrac{1}{3}] \quad (9)$$

$$E_{TH} = 3nRT \quad (10)$$

and

$$P_{TH} = -(dF_{TH}/dV)_T = \alpha_0 K_0 (T - T_0) \quad (11)$$

where α is the thermal expansivity, and we have used the fact that in the high-temperature limit, assuming that $q = 1$,

$$3nR\gamma_0/V_0 = C_V \gamma_0/V_0 = \alpha_0 K_0 \quad (12)$$

where C_v is the heat capacity at constant volume; $3nR$ is its high-temperature limiting value. Thus the assumed forms for the fundamental relation and equation of state for liquids are

$$\begin{aligned} F(V, T) &= F_0 + 9V_0 K_0[\tfrac{1}{2}f^2 + \tfrac{1}{3}a_1 f^3 + \tfrac{1}{4}a_2 f^4 + \cdots] \\ &\quad + 3nR[T \ln (\theta/T) - T_0 \ln (\theta_0/T_0) + (T - T_0)/3] \end{aligned} \quad (13)$$

and

$$\begin{aligned} P(V, T) &= -(dF/dV)_T \\ &= P_c(V, T_0) + P_{TH}(T - T_0) \\ &= 3K_0 f(1 + 2f)^{5/2}[1 + a_1 f + a_2 f^2 + \cdots] \\ &\quad + \alpha_0 K_0 (T - T_0) \end{aligned} \quad (14)$$

Not only is this simplification based on reasonable physical assumptions, but it results in a thermal pressure which is independent of volume, allowing the complete equation of state to be defined by only one parameter, α_0, in addition to the three Birch-Murnaghan parameters. This is important for liquids since constraints on the parameters, that is, experimental measurements of thermodynamic properties, are generally fewer and more uncertain than for solids.

Although the liquid equation of state (14) is simple and contains only four parameters (V_0, K_0, K_0', α_0), it shares with the full Mie-Grüneisen form (7) the rich behavior commonly exhibited by condensed matter equations of state. Thus (14) is consistent with a large body of experimental work on materials, including silicates, which documents not only compression and thermal expansion but also the increase of K with pressure [*Birch*, 1952], its decrease with temperature [e.g., *Isaak et al.*, 1989], the decrease of α with

pressure [e.g., *Chopelas and Boehler*, 1989], and its increase with temperature [*Skinner*, 1966] (Figure 1; see also *Vinet et al.* [1987]). This represents a distinct advantage over perturbative schemes, either simple polynomials in pressure and temperature or more complex forms [*Ohtani*, 1983; *Bottinga*, 1985; *Lange and Carmichael*, 1987; *Agee and Walker*, 1988; *Rigden et al.*, 1989; *Fei et al.*, 1990; *Plymate and Stout*, 1989, and references therein], which require an additional, often poorly constrained, parameter for each higher-order derivative property, such as the temperature dependence of K or the pressure dependence of α. Although such equations of state are useful at low compressions because the volume can often be written as an explicit function of T and P, successful application to the large compressions (exceeding $V/V_0 = 0.9$) of interest here apparently requires at least two parameters in addition to those used in (14) (the temperature derivatives of α and K) [*Plymate and Stout*, 1989].

While (14) has not previously been applied to silicate liquids, it has been used to successfully describe the equation of state of solid NaCl [*Birch*, 1986]. Moreover, the form of the thermal pressure assumed here is known to be an excellent approximation for a wide range of solids at high temperature ($T > \theta$) [*Anderson et al.*, 1982; *Vinet et al.*, 1987]. Finally, *Schlosser and Ferrante* [1989] have reproduced a subset of liquid alkali metal equation of state data using an identical form for P_{TH} and a slightly different form for P_c [*Vinet et al.*, 1986]. We now show, by comparison with experimental data, that (14) gives an excellent description of the equations of state of liquids over a wide range of pressure and temperature.

The Liquid Fundamental Relation

Liquid Alkali Metals

The liquid alkali metals are among the most studied liquids because of their low freezing points. They are ideal for equation of state studies because their low bulk moduli permit accurate measurements over a wide range of compression. The four necessary model parameters, V_0, K_0, K_0', and α_0, along with the assumed reference temperature, T_0, for sodium, potassium, rubidium, and cesium are taken from the ultrasonic measurements and review of thermodynamic data by *Shaw and Caldwell* [1985] and are listed in Table 1.

Figure 2 shows the excellent agreement between the model and the pressure measurements of *Makarenko et al.* [1977] along four different isotherms of potassium liquid. These four curves can be represented in a more convenient form which also serves as a further test of the model. Since

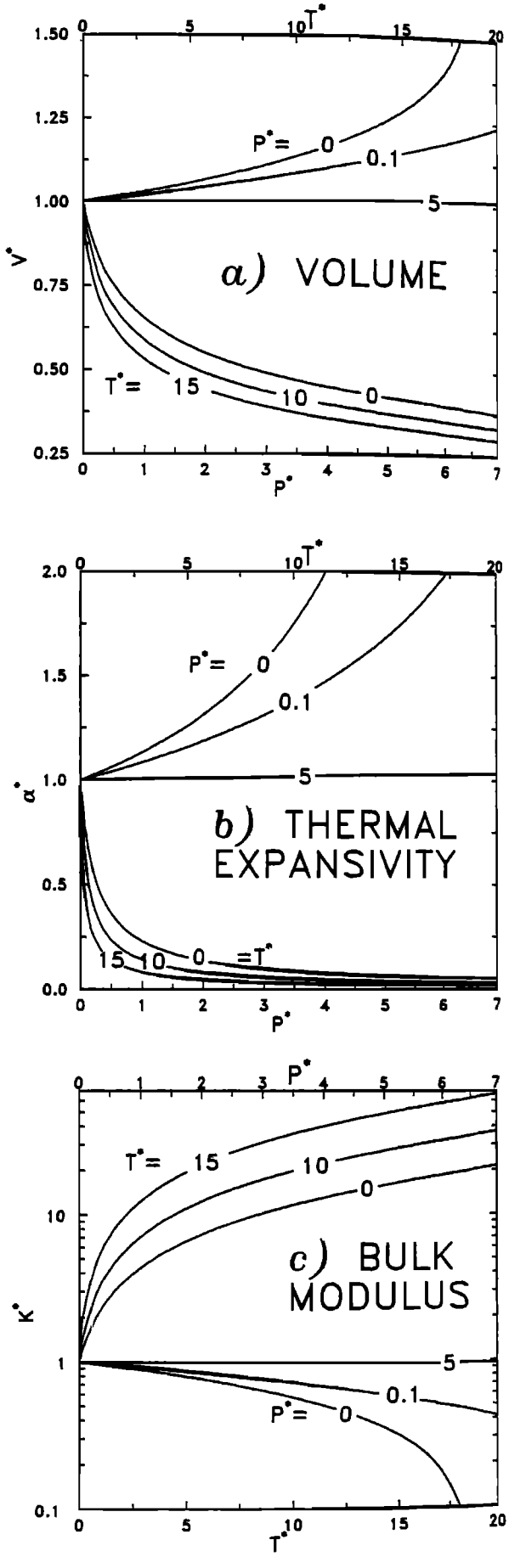

Fig. 1. (Opposite) Properties of the liquid equation of state (14) derived here, including the temperature and pressure variations of (*a*) volume, (*b*) thermal expansion, and (*c*) bulk modulus (note the logarithmic axis). For illustrative purposes we have assumed a second-order Birch-Murnaghan form ($K_0' = 4$) for which all the thermodynamic properties depend only on a scaled pressure, $P^* = P/K_0$, and a scaled temperature, $T^* = 100\alpha_0(T - T_0)$. The other scaled variables X^* (V^*, α^*, and K^*) are defined by $X/X(P_0 = 0, T^*)$ for isotherms and by $X/X(P^*, T_0)$ along isobars. The maximum plotted values of T^* and P^* are chosen to be slightly larger than the maximum values encountered in the Earth's mantle assuming $T_{max} = 5000$ K, $P_{max} = 140$ GPa, $K_0 = 20$ GPa, and $\alpha_0 = 6 \times 10^{-5}$ K^{-1} (see Table 1).

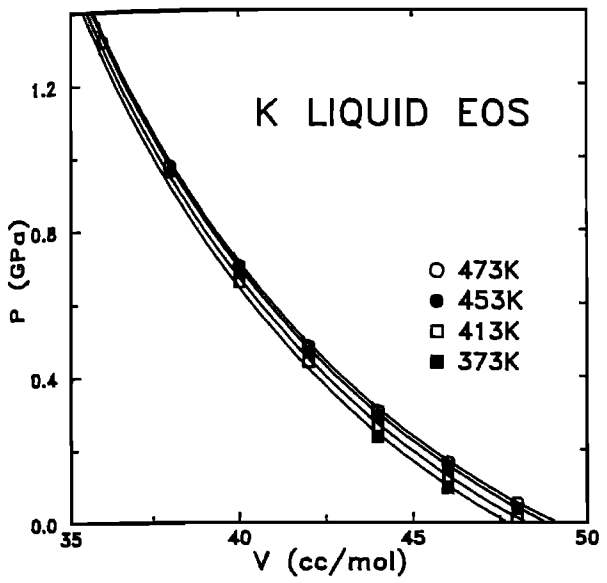

Fig. 2. Volume of potassium liquid as a function of pressure for four different temperatures predicted by the liquid equation of state (14) (curves) compared with the measurements of *Makarenko et al.* [1977] (symbols).

our model predicts that the variation of pressure with temperature at fixed volume is due only to the thermal pressure, the full equation of state for any substance can be represented as a single line by plotting the volume against a reduced pressure: the total pressure, P_{TOT}, minus the thermal pressure, P_{TH}. If the model is correct, experimental data from different isotherms should fall on a single line after the model thermal pressure is subtracted from the experimental (total) pressure. Figure 3, summarizing all the liquid alkali metal equation of state measurements of *Makarenko et al.* [1977], shows that this is indeed the case, providing further evidence of the model's accuracy.

We have also compared the temperature dependence of the bulk modulus predicted by the model with the measurements of *Shaw and Caldwell* [1985]. Figure 4 shows the excellent agreement between model and experiment. This figure also emphasizes the fact that our model does not require an additional parameter to produce the temperature dependence of the bulk modulus but incorporates it implicitly (see also Figure 1).

Water

While the bonding in alkali metals is relatively simple, the bonding in water, as in silicates, is more complex, containing significant covalent character. This, combined with the extremely large range in temperature and pressure over which the equation of state has been measured, makes water an ideal test for our model. For the assumed reference temperature of 373 K, V_0 and α_0 were taken from the steam tables [*Harr et al.*, 1984]. K_0 was calculated from the adiabatic bulk modulus, K_s, measured ultrasonically at T_0 by *Smith and Lawson* [1954], via the relation

$$1/K_0 = 1/K_{s0} + T_0 V_0 \alpha_0^2 / C_{p0} \quad (15)$$

where the heat capacity at constant pressure, C_p, was taken from the steam tables. Low-pressure ($P < 1$ GPa) equation of state data [*Grindley and Lind*, 1971] were fit to obtain K_0' and K_0''. A fourth-order Birch-Murnaghan equation of state was used because it fit the low-pressure data significantly better than a third order equation of state. The values of all the parameters are shown in Table 1.

A plot of the full equation of state of water from the model (Figure 5) shows the excellent agreement with data. Even though no data from above 1 GPa were used to constrain the model, it accurately predicts even the shock wave measurements [*Lyzenga et al.*, 1982] at nearly threefold compression and several thousands of degrees temperature. The model's success over this extreme range of conditions is important because, when scaled to the material properties of water, the ranges in temperature (maximum $T^* = 360$) and pressure (maximum $P^* = 39$) greatly exceed those encountered in the Earth's mantle (see Figure 1).

Silicate Liquids

Recently, extensive compilations of volume, thermal expansivity, and bulk modulus measurements [*Lange and Carmichael*, 1987] have combined with shock wave experiments on silicate liquids [*Rigden et al.*, 1984, 1988, 1989] to make predictions of silicate liquid equations of state feasible. While zero-pressure measurements of V, α, and K provide

TABLE 1. Parameters of the Fundamental Thermodynamic Relation: Liquids

Liquid	T_0, K	$-F_0$, kJ/mol	V_0, cm^3/mol	K_0, GPa	K_0'	θ_0, K	α_0, 10^{-5} K^{-1}
Enstatite	1773	254.6 (1)[a]	38.73 (08)[b]	21.3 (2.1)[b]	6.4 (5)[c]	625 (4)[a]	5.47 (2.97)[b]
Diopside	1773	521.1 (1)[a]	82.45 (15)[b]	23.2 (2.0)[b]	6.4 (5)[c]	632 (4)[a]	7.29 (2.35)[b]
Sodium[d]	382.4	···	24.873	5.33	3.7	···	23.8
Potasium[d]	357.8	···	47.519	2.57	4.1	···	26.9
Rubidium[d]	333.1	···	58.181	2.06	3.9	···	27.4
Cesium[d]	322.7	···	72.693	1.57	3.8	···	28.4
Water	373	···	18.797[e]	2.06[f]	6.29[g]	···	73.5[e]

Uncertainties in the last digits reported are given in parentheses.
[a] *Stebbins et al.* [1984].
[b] *Lange and Carmichael* [1987].
[c] Estimated by *Duffy and Anderson* [1989].
[d] *Shaw and Caldwell* [1985].
[e] *Harr et al.* [1984].
[f] *Smith and Lawson* [1954].
[g] $K_0 K_0'' = -1.89$; *Grindley and Lind* [1971].

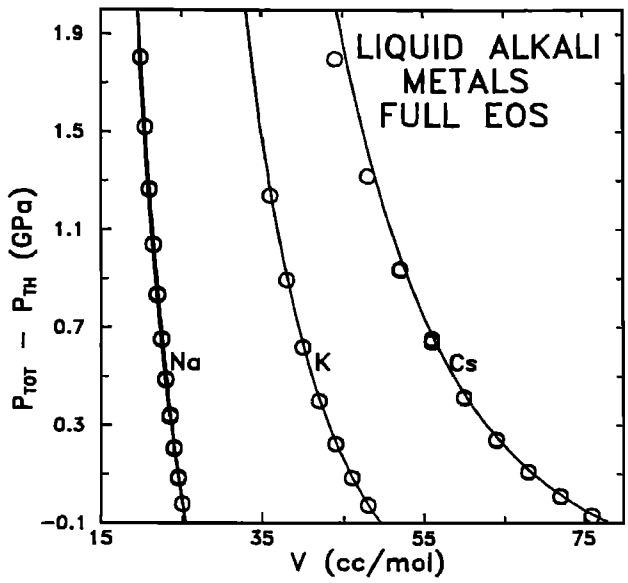

Fig. 3. Volume of the alkali metal liquids plotted against the total pressure P_{TOT} minus thermal pressure P_{TH} predicted by the liquid equation of state (14) (curves), compared with the measurements of *Makarenko et al.* [1977] (circles). The experimental points, which consist of several nearly coincident points measured at different temperatures, are plotted by subtracting the model's thermal pressure (P_{TH}) at the experimental volume and temperature from the experimental pressure (P_{TOT}). The deviation of the two highest pressure cesium points may be due to a pressure-induced electronic transition in this liquid [e.g., *Simozar and Girifalco*, 1983].

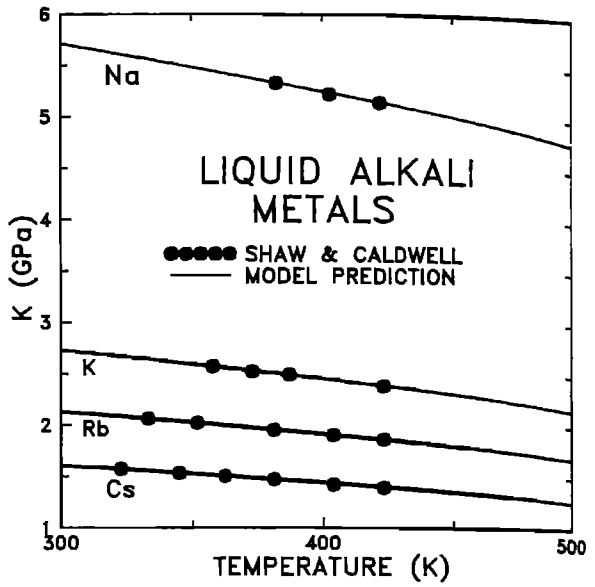

Fig. 4. Temperature dependence of the bulk modulus of the liquid alkali metals predicted by the liquid equation of state (14) (lines) compared with the measurements of *Shaw and Caldwell* [1985] (circles).

us with the necessary equation of state parameters (except K', which we estimate below), the shock wave measurements provide a test of our model. Although the $MgSiO_3$ composition, of primary interest here, has not yet been measured by shock techniques, we will compare our model's predictions with shock measurements on $CaMgSi_2O_6$, a similar pyroxene composition.

The parameters V_0, K_0, and α_0 for both diopside and enstatite compositions are taken from *Lange and Carmichael* [1987]. To estimate K_0', we use the solid state systematics of *Duffy and Anderson* [1989]. Value of these parameters are listed in Table 1. We use solid state systematics since data on K_0' for silicate liquids is only rarely available [e.g., *Rigden et al.*, 1989]. The systematics provide a consistently uniform approach for both enstatite and diopside liquids as well as enstatite and ilmenite crystals. Although such estimates are potentially crude, the resulting model equation of state is in excellent agreement with the shock wave data (Figure 6) for diopside liquid. This gives us confidence that the estimate of K_0' for the similar $MgSiO_3$ composition will also lead to an accurate equation of state. We note that the systematics-derived K_0' for enstatite agrees with the estimate of *Rigden et al.* [1989], who find $K_0' = 6.8 \pm 1.5$. Our smaller uncertainty of ± 0.5 is derived from the solid state systematics.

While it is likely that diopside liquid undergoes a gradual pressure-induced fourfold to sixfold Si-O coordination change within the experimental pressure range (on the basis of spectroscopic measurements the coordination change is complete below 30 GPa in silicate liquids [*Williams and Jeanloz*, 1988]), the excellent agreement between model and experiment suggests that a single set of parameters is capable of describing compression in both low-pressure, tetrahedral and high-pressure, octahedral regimes (see also *Rigden et al.* [1989]). Like diopside liquid, anorthite liquid also appears to compress normally while undergoing the coordination change: shock data on this composition (up to 35 GPa) are also readily explained by the Birch-Murnaghan equation [*Rigden et al.*, 1989]. This is in contrast to the well-known

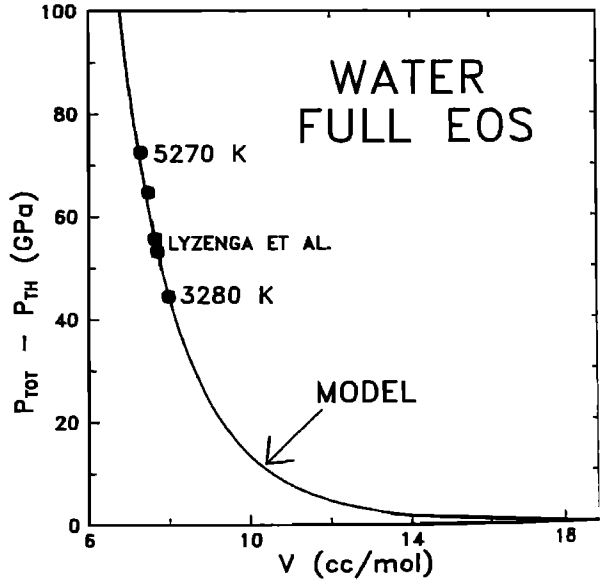

Fig. 5. Volume of water plotted against the total pressure P_{TOT} minus the thermal pressure P_{TH} predicted by the liquid equation of state (14) (curve), compared with the shock wave measurements of *Lyzenga et al.* [1982] (circles). The range of experimentally measured temperatures is indicated. The experimental points are plotted by subtracting the model's thermal pressure (P_{TH}) at the experimentally measured volume and temperature from the experimental pressure (P_{TOT}).

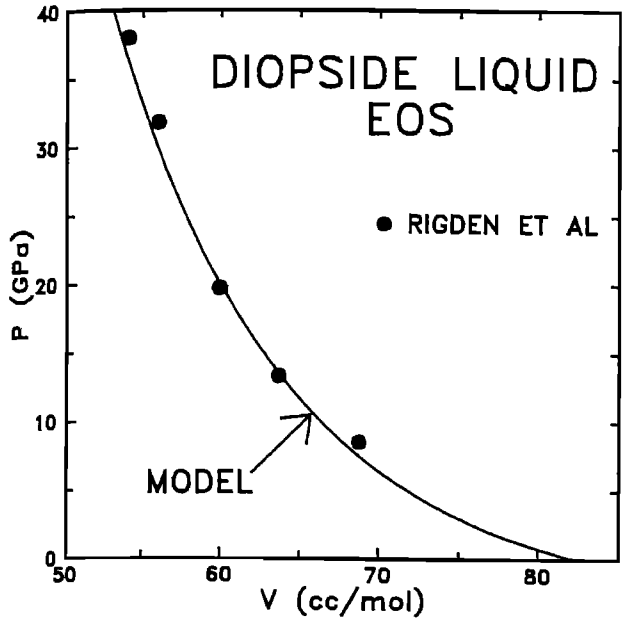

Fig. 6. Volume of diopside liquid as a function of pressure predicted by the liquid equation of state (14) (curve) at $T = 1773$ K, compared with the shock wave measurements of *Rigden et al.* [1989] (circles). The excellent agreement shows not only the ability of the Birch-Murnaghan equation of state to describe the liquid's compression (which has been noted previously by *Rigden et al.* [1989]) but also the accuracy of our estimate of K_0' from solid-state systematics (see text).

behavior of crystals (compare V_0, K_0, and K_0' of tetrahedral enstatite and octahedral perovskite, Table 2) and to a particular model of silicate liquid compression which predicts a rapid decrease in compressibility (stiffening) of the liquid once the coordination change is completed [*Stolper and Ahrens*, 1987; *Rigden et al.*, 1988]. Although diopside and anorthite liquids show no evidence of rapid stiffening, an anorthite-diopside mixture does (onset of stiffening occurs at around 25 GPa [*Rigden et al.*, 1988]). Rapid stiffening has also been invoked to explain perovskite melting data, but with a much higher onset pressure of 60 GPa [*Knittle and Jeanloz*, 1989*a*]. However, the anomalous behavior of the anorthite-diopside mixture may be due instead to vitrification or crystallization in the shock experiment [*Rigden et al.*, 1988], while the perovskite melting data are equally well explained by a liquid which compresses normally, in accordance with our model (see *Knittle and Jeanloz* [1989*a*] and the discussion of perovskite melting below). Because existing data are inconclusive and, in the case of diopside and anorthite liquid compression, appear to favor our simple model over one which predicts rapid stiffening, we retain the assumption that our equation of state with a single set of parameters (V_0, K_0, K_0', α_0) is sufficient to describe the compression of a silicate liquid throughout the Earth's pressure-temperature regime.

We obtained the remaining fundamental relation parameters, F_0 and θ_0, for the $MgSiO_3$ and $CaMgSi_2O_6$ liquids by requiring that the calculated zero-pressure melting point and the zero-pressure entropy of melting agreed with the experiment (Table 1). The parameter γ_0 is not independent in the liquid fundamental relation but is given by

$$\gamma_0 = V_0 K_0 \alpha_0 / 3nR \tag{16}$$

Thus the silicate liquid fundamental relations are completely determined without reference to melting data at pressures greater than zero. The good agreement between predicted and experimental melting curves for both $CaMgSi_2O_6$ and $MgSiO_3$ compositions, described below, provides further evidence of the accuracy of the fundamental relation model for silicate liquids.

The Solid Fundamental Relation

The six defining parameters, F_0, V_0, K_0, K_0', γ_0, and θ_0, were constrained by high-pressure X ray and ultrasonic measurements and thermal expansivity and thermochemical data on the four minerals considered here: diopside, enstatite, ilmenite, and perovskite. All parameters are listed in Table 2. V_0 is taken from single-crystal X ray measurements for all the minerals. K_0 values for enstatite, ilmenite, and diopside were taken from ultrasonic measurements, while that for perovskite was taken from the high-pressure volume measurements of *Knittle and Jeanloz* [1987]. Compression studies also provided K_0' for diopside and perovskite, while for ilmenite this quantity was estimated from solid-state systematics [*Duffy and Anderson*, 1989]. Although K_0' for enstatite has been measured by high-pressure ultrasonic techniques, it was found to be anomalously high, 9.5–11.6 [*Frisillo and Barsch*, 1972; *Webb and Jackson*, 1985], compared with more typical values of 3–6 [*Jeanloz*, 1989]. However, the value of $-K_0K_0''$ (≈ 155) was also found to be anomalously large; the third-order Birch-Murnaghan equation predicts $-K_0K_0'' = 40$ for $K_0' = 9.5$ (see, for example, *Jeanloz* [1988]). Because of the large experimental uncer-

TABLE 2. Parameters of the Fundamental Thermodynamic Relation: Crystals

Mineral	T_0, K	F_0, kJ/mol	V_0, cm^3/mol	K_0, GPa	K_0'	θ_0, K	γ_0
Enstatite	300	0	31.33 (1)[a]	106 (1)[b]	5.0[c]	935 (4)[d]	0.974 (19)[d]
Ilmenite	300	60.97 (1)[d]	26.35 (1)[e]	212 (2)[f]	4.3[c]	1026 (10)[d]	1.480 (36)[d]
Perovskite	300	102.24 (1)[g]	24.46 (1)[h]	266 (6)[i]	3.9 (4)[j]	1012 (6)[g,j]	1.73 (14)[g,j]
Diopside	300	0	66.11 (3)[k]	114 (1)[l]	4.5 (5)[m]	941 (5)[k,n]	1.062 (15)[k,n]

Note that $q = 1$ (1) for all materials. Uncertainties in the last digits reported are given in parentheses.
[a] *Sasaki et al.* [1982].
[b] *Weidner et al.* [1978].
[c] Estimated by *Duffy and Anderson* [1989].
[d] *Ashida et al.* [1988].
[e] *Horiuchi et al.* [1982].
[f] *Weidner and Ito* [1985].
[g] *Ito and Takahashi* [1989].
[h] *Ross and Hazen* [1989].
[i] *Knittle and Jeanloz* [1987].
[j] *Knittle et al.* [1986].
[k] *Finger and Ohashi* [1976].
[l] *Levien et al.* [1979].
[m] *Levien and Prewitt* [1981].
[n] *Krupka et al.* [1985].

TABLE 3. Parameter Uncertainties Using Partial Information

Mineral	Thermal Expansivity				Heat Capacity			
	θ_0, K	$\sigma(\theta_0)$, K	γ_0	$\sigma(\gamma_0)$	θ_0, K	$\sigma(\theta_0)$, K	γ_0	$\sigma(\gamma_0)$
Enstatite	640	1145	0.86	0.12	943	5	1.064	0.029
Ilmenite	17	360	1.22	0.04	991	11	0	0.25
Perovskite	2720	1700	3.9	3.3	...	...	...	...
Diopside	670	1110	1.02	0.13	925	6	0.900	0.042

Note that $\sigma(X)$ is the uncertainty in X at the 65% confidence level. The columns headed thermal expansivity are due to constraining the parameters with thermal expansivity data alone. The columns headed heat capacity are due to constraining the parameters with heat capacity data alone.

tainties in K_0' and K_0K_0'', and because the large negative value of K_0K_0'' will cause K' to reach more typical values rapidly with pressure (see also *Webb and Jackson* [1985]), we represented enstatite compression by a third-order Birch-Murnaghan equation with K_0' calculated from solid-state systematics [*Duffy and Anderson*, 1989]. What is important is that the Birch-Murnaghan equation gives accurate densities at all relevant pressures. With the K_0' value derived from systematics, it gives densities that are consistent with shock wave data [*Watt and Ahrens*, 1986] and high-pressure X ray diffraction studies [*Olinger*, 1977; *Ralph and Ghose*, 1980].

The thermal parameters γ_0 and θ_0 were constrained by simultaneously fitting to thermal expansion and heat capacity data for enstatite, ilmenite, and diopside, while for perovskite, thermal expansion data were combined with the measured slope of the ilmenite-perovskite transition boundary. Since no heat capacity data are available for $MgSiO_3$ perovskite, it is interesting to note that our θ_0 is generally consistent with, though somewhat lower than, a theoretical value based on lattice dynamics calculations [*Bukowinski and Wolf*, 1988] and an estimate from systematics [*Watanabe*, 1982], both of which give a value of about 1200 K. We use our current estimate since it is based on measured properties of perovskite. Thermal expansion was calculated from the equation of state (7) while the heat capacity C_P was calculated from the fundamental relation (1)–(6) and the identity

$$C_P = C_V + C_V^2\gamma^2 T/Kv \tag{17}$$

where

$$C_V = -T\,(d^2F/dT^2)_V = 9nR(T/\theta)^3 \int_0^{\theta/T} e^t t^4\, dt/(e^t - 1)^2 \tag{18}$$

The ilmenite-perovskite phase transition slope is calculated from the Clasius-Clapeyron equation:

$$(dP/dT)_{eq} = (S_2 - S_1)/(V_2 - V_1) \tag{19}$$

where the entropy S is given by the fundamental relation (1)–(6)

$$S = -(dF/dT)_V = 9nR(T/\theta)^3 \cdot \int_0^{\theta/T} [t(e^t - 1)^{-1} - \ln(1 - e^{-t})]t^2\, dt \tag{20}$$

near the center of the experimental range at 23.7 GPa and 1600 K [*Ito and Takahashi*, 1989].

The optimal parameters were found by minimizing the chi-square function:

$$X^2 = \sum_i (Y_i^{exp} - Y_i^{calc})^2/\sigma_i^2 \tag{21}$$

where Y_i^{exp} and σ_i are the measured properties and their uncertainties, respectively, and Y_i^{calc} are the calculated properties. In all cases the $X^2(\gamma_0, \theta_0)$ surface was found to be free of multiple minima so that nonlinear inverse methods such as the Levenberg-Marquardt algorithm [*Press et al.*, 1986, pp. 521–528] converged in about five iterations even for initial guesses twice the optimal values. Uncertainties in the parameters were determined by mapping the $X^2(\gamma_0, \theta_0)$ surface and are reported at the 68% confidence level [see *Press et al.*, 1986, p. 537]. In all cases our fitting procedure resulted in tight bounds on γ_0 and θ_0 (uncertainties not exceeding 8%; see Table 2), crucial for meaningful extrapolation to high pressure and temperature, while fits to either thermal expansion or heat capacity data alone resulted in parameter uncertainties which were often orders of magnitude larger (Table 3).

The excellent fit of the model to experiment (Figures 7–10) shows that the fundamental relation (1)–(6) is accurate and that the data do not require any anharmonic terms in the fundamental relation. Recently, perovskite thermal expansion data were inverted for not only γ_0 and θ_0 but also a nonzero anharmonic parameter [*Jeanloz and Knittle*, 1989]. Using the values determined by these authors, we calculate a X^2 value of 5.45 for the fit to thermal expansion data. However, the fact that our optimal fit with only two parameters (Table 2) is significantly better ($X^2 = 4.52$) and lies well within experimental uncertainties (Figure 10) indicates that the anharmonic parameter is not statistically different from zero.

The F_0 values for the three magnesium silicate minerals were determined relative to enstatite, assigned $F_0 = 0$, since only differences in F_0 can be constrained. F_0 for ilmenite was determined by combining the measured enstatite-ilmenite enthalpy (H) difference [*Ashida et al.*, 1988] with the difference in entropy calculated from the fundamental relation (20):

$$F_0(\text{il}) = [H(\text{il}) - H(\text{en})] - T[S(\text{il}) - S(\text{en})] \tag{22}$$

F_0 for perovskite was then obtained by requiring the calculated ilmenite-perovskite phase boundary to go through the measured point at 23.7 GPa and 1600 K. Phase boundaries were calculated by finding the set of pressure-temperature points at which the Gibb's free energy,

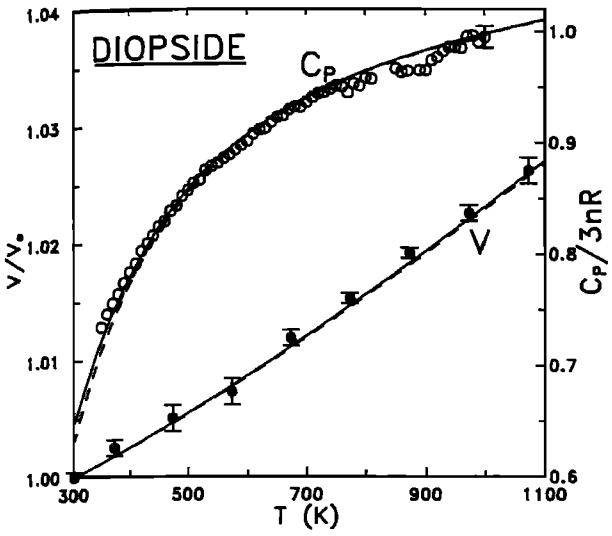

Fig. 7. Heat capacity at constant pressure and thermal expansion of diopside predicted by the solid fundamental relation (1)–(6) using the Debye model (solid curves) and Einstein model (dashed curves), compared with the experimental data of *Krupka et al.* [1985] and *Finger and Ohashi* [1976]. Reported uncertainties for the volume and heat capacity measurements are indicated by error bars. The characteristic temperatures of the Debye and Einstein models are related by $\theta_{0D} = (5/3)^{1/2}\theta_{0E}$ [*Wallace*, 1972].

$$G = F + PV \tag{23}$$

of the two phases were equal. The resulting F_0 values are given in Table 2, and the calculated $MgSiO_3$ solid phase equilibria, which are in excellent agreement with experiment, are shown in Figure 11.

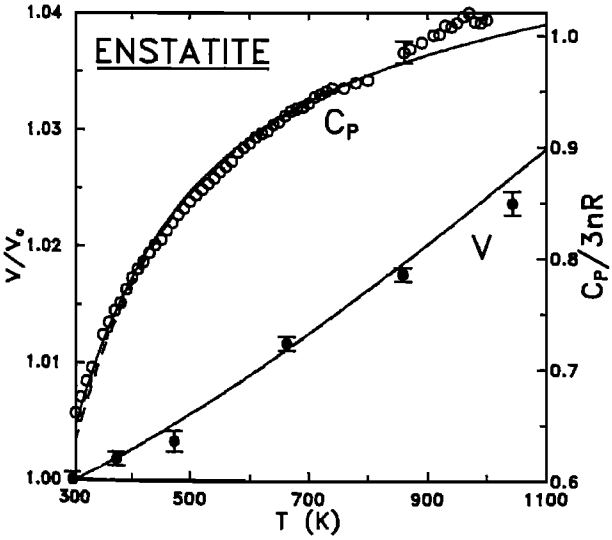

Fig. 8. Heat capacity at constant pressure and thermal expansion of ortho-enstatite predicted by the solid fundamental relation (1)–(6) using the Debye model (solid curves) and Einstein model (dashed curves; see Figure 7) compared with the experimental data of *Krupka et al.* [1985] and *Suzuki* [1975]. Reported uncertainties for the volume and heat capacity measurements are indicated by error bars.

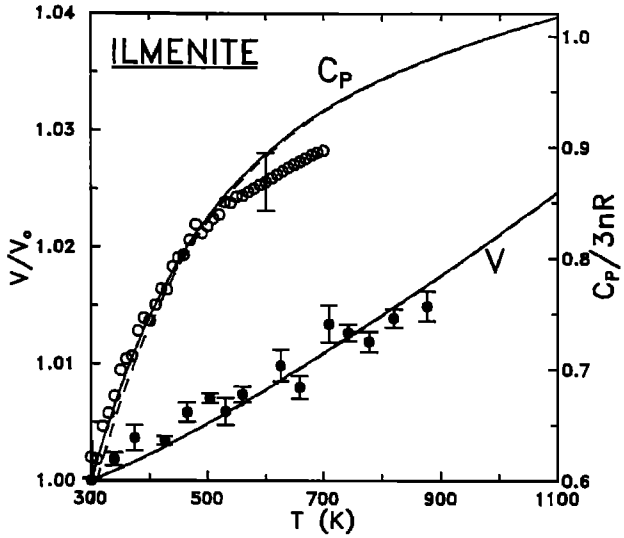

Fig. 9. Heat capacity at constant pressure and thermal expansion of ilmenite predicted by the solid fundamental relation (1)–(6) using the Debye model (solid curves) and Einstein model (dashed curves; see Figure 7) compared with the experimental data of *Ashida et al.* [1988]. Reported uncertainties for the volume and heat capacity measurements are indicated by error bars. The source of the systematic deviation of experimental heat capacity data from prediction above 600 K is not certain, since these are the only measurements of ilmenite heat capacity at these temperatures. However, *Ashida et al.* [1988] note that their measured enstatite heat capacity deviates systematically from the more precise measurements of *Krupka et al.* [1985] above 600 K. This suggests that the small deviation between model and data for ilmenite may be caused by systematic experimental error at high temperature.

Melting Curves and Geophysical Implications

Melting curves were calculated in the same way as the solid-solid phase boundaries described above, by equating Gibb's free energies of solid and liquid. Calculated melting curves for enstatite and diopside, shown in Figures 12 and 13, are in excellent agreement with experiment, even though no high-pressure ($P > 0$) melting data were used to constrain the fundamental relations. This gives us confidence not only in the form of the liquid and solid fundamental relations but also in the values of the parameters determined here. Sensitivity to parameter uncertainties was checked by varying the most uncertain parameter, K_0' of the liquid, by ± 0.5. The resultant variation in the melting curve is comparable to experimental uncertainties within the experimental pressure range and is large enough to accommodate the variations, mostly much smaller, due to uncertainties in all the other liquid and solid parameters.

The melting curve of perovskite, calculated throughout the pressure regime of the Earth's mantle, is shown in Figure 14. Although we overestimate the melting temperature between 50 and 80 GPa (by less than 270 K, or 8%), theory and experiment [*Heinz and Jeanloz*, 1987; *Knittle and Jeanloz*, 1989*a*] are in very good agreement within their combined uncertainties even though the calculations are completely independent of perovskite melting data. While the $MgSiO_3$ end-member is expected to melt at a higher temperature than the experimental substance, $Mg_{0.9}Fe_{0.1}SiO_3$, accounting for some of the discrepancy, the effect of Fe is expected to be small compared with experimental uncertainties: the effects of incongruency on the melting point were not measurable

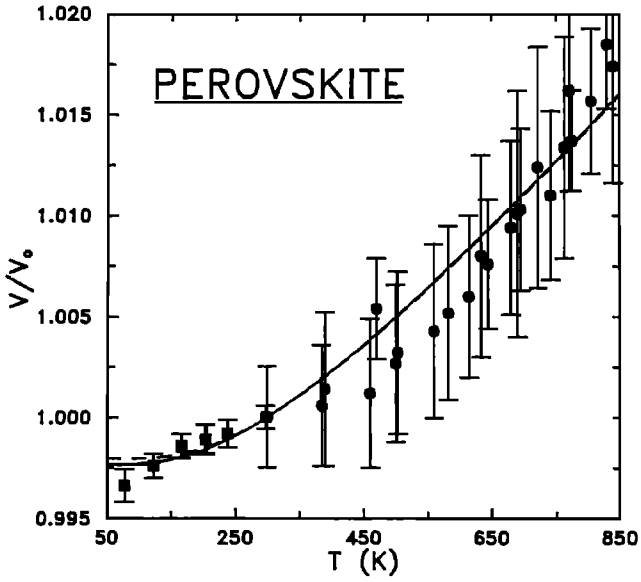

Fig. 10. Thermal expansion of perovskite predicted by the solid thermal equation of state (7) using the Debye model (solid curve) and Einstein model (dashed curve; see Figure 7) compared with the experimental data of *Knittle et al.* [1986] (circles). Reported uncertainties for the volume measurements are indicated by error bars. Also shown are the low-temperature data of *Ross and Hazen* [1989] (squares) which were not used in the inversion for perovskite thermal parameters. Nevertheless, the Debye model agrees with all but the lowest temperature measurement within experimental uncertainties. Note that the differences between the Debye and the Einstein models are only apparent at very low temperatures.

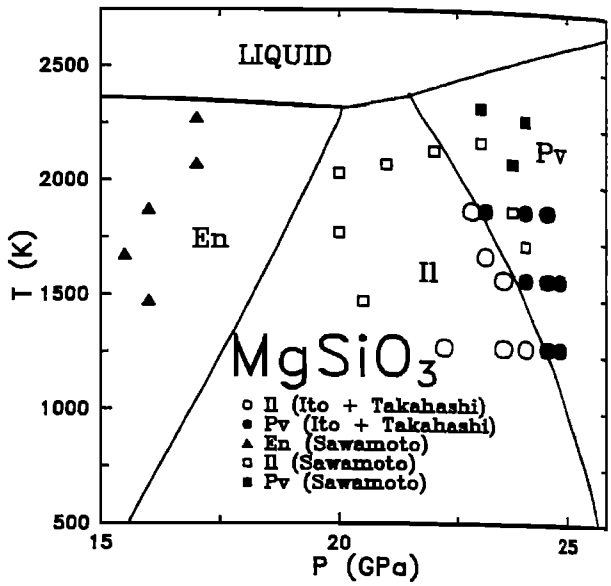

Fig. 11. $MgSiO_3$ phase diagram predicted by the model (lines) compared with the experimental observations of *Ito and Takahashi* [1989] and *Sawamoto* [1987]. The predicted phase diagram is in good agreement with observations of the phases considered here. Note that the ilmenite-perovskite phase boundary measured by *Sawamoto* [1987] is slightly discrepant with the later measurements of *Ito and Takahashi* [1989] which are used here to constrain the thermal parameters of perovskite. The transition boundaries shown here are uniquely determined by our analysis and are not affected by the existence of other phases known to reside in the enstatite-ilmenite gap, including fields of magnesium silicate spinel and stishovite; modified spinel and stishovite; and the liquidus phase between 20 and 25 GPa, tetragonal garnet [*Kato and Kumazawa*, 1985; *Sawamoto*, 1987], which is not considered here because there is insufficient data to constrain its fundamental relation.

[*Heinz and Jeanloz*, 1987; *Knittle and Jeanloz*, 1989*a*]. Uncertainties in the parameters lead to variations in the melting curve which are comparable to experimental uncertainties, reaching ±600 K at the base of the mantle.

The predicted melting point of $MgSiO_3$ perovskite at the core-mantle boundary (3750 ± 600 K) is substantially lower than previous estimates, based on either empirical melting laws or extrapolation of experimental data. Applications of the Kraut-Kennedy and Lindemann laws produce melting curves which are inconsistent [*Ohtani*, 1983] or marginally consistent [*Poirier*, 1989] with data and produce core-mantle boundary (CMB) melting temperatures 1300–4000 K higher than our prediction. *Knittle and Jeanloz* [1989*a*] hypothesized that the perovskite melting curve increases its dT/dP slope rapidly at high pressure, because of rapid stiffening of the liquid equation of state, leading to an extrapolated CMB melting point of 4500 K. However, the melting slope of a single phase almost universally decreases with pressure [*Liu and Bassett*, 1986] (plutonium is apparently an exception to this rule), and *Knittle and Jeanloz* [1989*a*] noted that their data were also consistent with a normal melting curve such as the one predicted here.

The main difference between our perovskite melting curve and previous estimates is that the dT/dP melting slope in our calculations decreases steadily with pressure, eventually becoming negative. That is, the density of the liquid approaches and eventually surpasses that of the crystal for all of the minerals studied here (see (19)). Although they have not yet been observed experimentally in one-component silicate systems, negative melting slopes are not uncommon in general [*Liu and Bassett*, 1986] (water is the most familiar

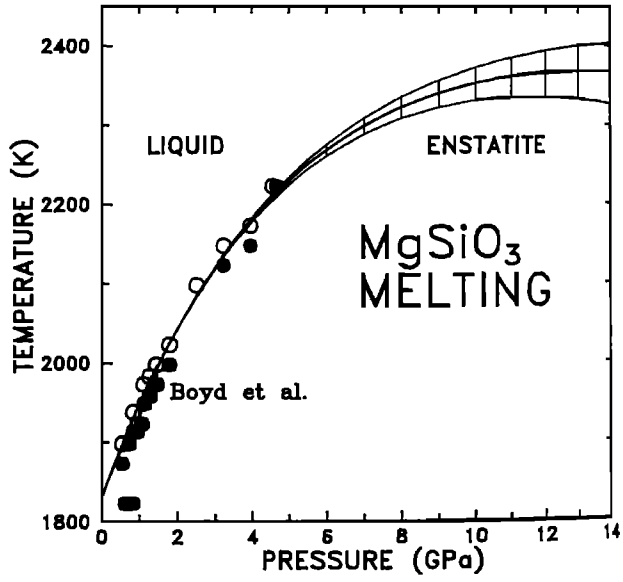

Fig. 12. Melting curve of ortho-enstatite predicted here (curves) compared with the experimental data of *Boyd et al.* [1964]. The open circles represent experimental observation of liquid, and the solid circles represent observation of solid. The hatched area represents uncertainties in the predicted melting curve (see text).

example), and the liquidi of some complex silicate systems such as peridotite [*Takahashi*, 1986] display liquidus maxima.

Although our approach is thermodynamic and therefore unable to provide unique structural information, we can think of the melting maxima of four-coordinated solid phases as being caused by gradual pressure-induced Si-O coordination increases in the liquid from fourfold to sixfold. This argument follows naturally from the fact that crystalline silicates all undergo fourfold to sixfold coordination changes at high pressure [*Liu and Bassett*, 1986] and is supported by recent spectroscopic measurements of high-pressure silicate liquids and glasses [*Williams and Jeanloz*, 1988; *Xue et al.*, 1989]. Since Si-O coordinations higher than six are unknown in silicates, the melting maxima of six-coordinated ilmenite and perovskite are more difficult to interpret in terms of liquid structure. However, since a liquid is not constrained to long-range order, it is able to adopt a wide range of structures unavailable to the crystal. This structural freedom may allow the liquid to respond more effectively to pressure and thus to become denser than the crystal even without undergoing an increase in coordination. This idea is supported by Monte Carlo simulations which show that the density of a four-coordinated silicate liquid can surpass that of the densest four-coordinated crystalline phases without increasing its coordination [*Stixrude and Bukowinski*, 1989].

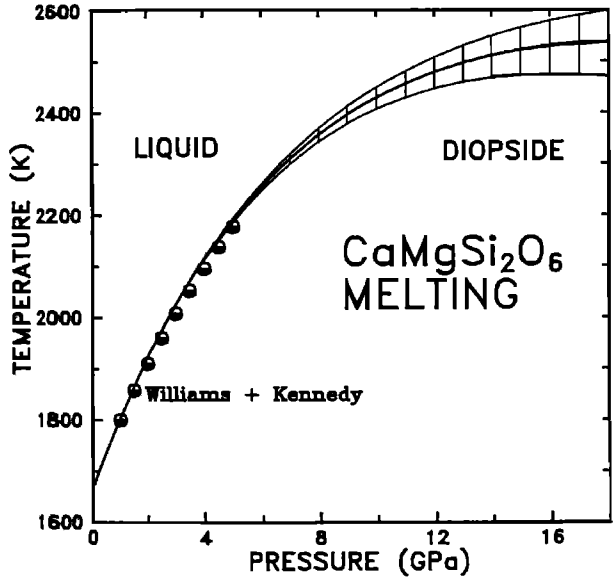

Fig. 13. Melting curve of diopside predicted here (curves) compared with the experimental data of *Williams and Kennedy* [1969] without corrections for thermocouple emf (symbols). The hatched area represents uncertainties in the predicted melting curve (see text). The uncertain thermocouple emf corrections increase the experimental melting temperatures by as much as 43 K at 5 GPa. Not shown are the data of *Boyd and England* [1963] and *Boettcher et al.* [1982]. These two data sets are consistent with our calculations and with the data of *Williams and Kennedy* [1969] below about 3 GPa, the highest pressure measured by *Boettcher et al.* [1982]. At higher pressures, Williams and Kennedy believe that the melting temperatures of Boyd and England, which fall as much as 53 K below our predicted curve at 4.67 GPa, are systematically underestimated. The data of *Scarfe and Takahashi* [1986] fall well below the predicted curve, by as much as 200 K at 13 GPa, but reaction with the graphite capsule may cause these temperatures to be underestimated [*Scarfe and Takahashi*, 1986].

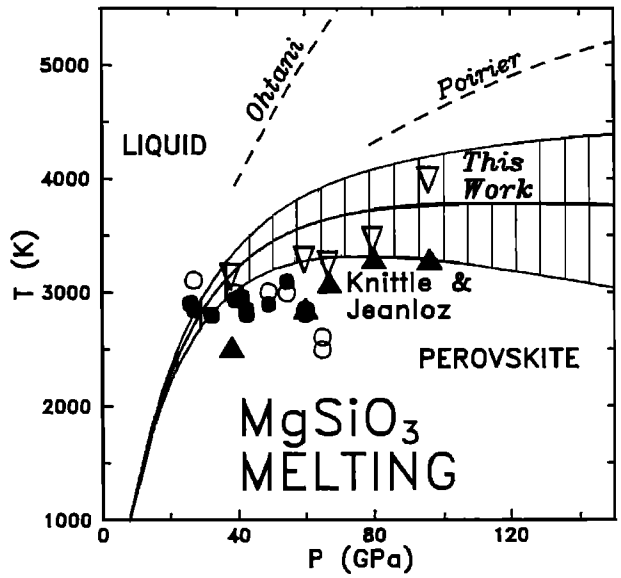

Fig. 14. Melting curve of perovskite predicted here (curves) compared with the experimental data of *Knittle and Jeanloz* [1989*a*] (triangles) and *Heinz and Jeanloz* [1987] (circles). The open and solid symbols represent observations of liquid and solid, respectively, and for the data of *Knittle and Jeanloz* [1989*a*] the upward and downward pointing symbols represent experimental brackets on the melting point (including uncertainties in temperature) at each pressure. The hatched area represents uncertainties in the predicted melting curve (see text). The two highest pressure points of *Heinz and Jeanloz* [1987], which are discrepant with both our prediction and the later measurements of *Knittle and Jeanloz* [1989*a*], are probably biased [*Knittle and Jeanloz*, 1989*a*]. Also shown are previous predictions of the perovskite melting curve, made by *Ohtani* [1983] and *Poirier* [1989].

Thus although it is possible that Si-O coordinations higher than six occur in silicates at extreme pressures, it seems unnecessary to postulate them to explain the perovskite and ilmenite melting maxima predicted here.

The locations of the predicted liquid-crystal density inversions are determined almost entirely by pressure with the increase in temperature along the melting curve playing a minor role. Isothermal compression at the zero-pressure melting temperature accounts for nearly all of the decrease in the volume of fusion (Figure 15). Thus from a thermodynamic standpoint, liquid-crystal density inversions in our calculations are simply a result of the liquid's much greater compressibility (Tables 1 and 2).

This simple relationship between liquid-crystal compressibility contrast and liquid-crystal density inversion suggests that perovskite, a possible liquidus phase at lower mantle pressures [*Ohtani*, 1983], may float in coexisting liquid deep in the Earth: although natural magmatic compositions are more complex than the one-component systems studied here, silicate liquid compressibility is a weak function of composition [*Rivers and Carmichael*, 1987]. Liquid-crystal density inversions in natural multicomponent systems will also be influenced by element partitioning, especially of Fe, between solid and melt. However, if Fe behaves as an incompatible element throughout the Earth as it does at lower pressure [*Heinz and Jeanloz*, 1987; *Ito and Takahashi*, 1987; *Kato et al.*, 1989], it will tend to increase the liquid's density relative to the solid. Thus the early evolution of the lower mantle and core-mantle boundary region as well as the

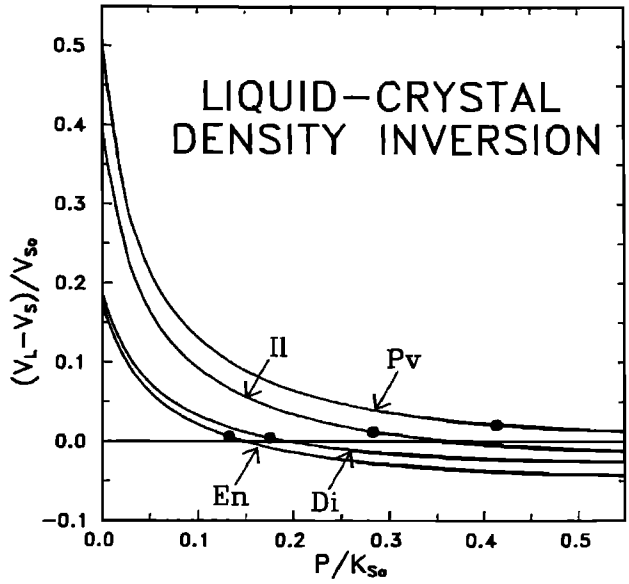

Fig. 15. Reduction of the liquid-crystal volume difference ($V_L - V_S$) due to isothermal compression at the liquid reference temperature (T_0 = 1773 K) calculated for the four minerals considered here (curves). The volume difference is normalized in each case to V_0 of the solid, and the pressure is normalized to K_0 of the solid. The circles mark the pressure at which the volume of melting for that mineral vanishes.

upper mantle [*Stolper et al.*, 1981; *Nisbet and Walker*, 1982] and transition zone [*Ohtani*, 1988; *Anderson and Bass*, 1986] may have been strongly influenced by liquid-crystal density inversions (see also *Ohtani* [1983]).

Constitution of the *D*″ Layer

Our predicted perovskite melting curve lies well above proposed geotherms [*Jeanloz and Morris*, 1986] throughout most of the lower mantle, thought to be composed mostly of (Mg, Fe)SiO_3 perovskite and a smaller amount of (Mg, Fe)O magnesiowüstite [*Bukowinski and Wolf*, 1990], and is therefore consistent with the lack of widespread melting required by seismic observations [*Lee and Johnson*, 1984] (Figure 16). However, in the *D*″ region at the base of the mantle, geotherms based on recent estimates of the temperature at the top of the core (4500–5500 K [*Williams and Jeanloz*, 1990]) exceed our predicted melting curve by as much as 1200 K. If we accept these estimates, our results imply that perovskite cannot be a constituent of *D*″ since the perovskite melting curve places an upper temperature bound on its stability regardless of other phases which may be present.

Thus although we will assume for simplicity that the chemical composition of *D*″ is similar to the lower mantle (i.e., Mg, Fe, and Si oxides are its major components, rather than, for example, Ca and Al oxides [*Ruff and Anderson*, 1980]), its phase assemblage must be very different. At *D*″ pressure-temperature conditions the (Mg, Fe)SiO_3 component of the mantle will, unless we invoke an as yet undiscovered postperovskite silicate phase, either partially melt or, if its constituent oxides have sufficiently high melting points, dissociate to magnesiowüstite and silica (in the form of either stishovite or its recently discovered high-pressure modification [*Tsuchida and Yagi*, 1989]).

However, seismic observations make a partially molten *D*″ unlikely. Partial melting will cause a large reduction in shear wave velocity since silicate liquids have a vanishingly small shear modulus at seismic frequencies [*Rivers and Carmichael*, 1987]. Although the seismic properties of *D*″ are highly variable [*Young and Lay*, 1987], there is no evidence for a sharp reduction of *S* wave velocity at the lower mantle–*D*″ boundary. Further, although there is some evidence for a more gradual reduction of *S* and *P* wave velocities with depth in *D*″, an increase in the amount of partial melt with depth would cause a much larger reduction than is observed: a temperature increase of 1000 K across a *D*″ of lower mantle mineralogy and composition accounts for the seismic observations [*Agnon and Bukowinski*, 1988].

A *D*″ layer consisting of magnesiowüstite and silica, a return to *Birch*'s [1952] original suggestion that silicates dissociate to simple oxides deep in the Earth, is consistent both with our results and with seismic observations. While magnesiowüstite will tend to lower seismic velocities, silica will tend to raise them, consistent with the small differences between spherically averaged *D*″ and lowermost mantle velocities [*Dziewonski and Anderson*, 1981]. This is because the bulk and shear moduli of stishovite, and probably its very similar high-pressure modification as well, are higher than those of perovskite, while the moduli of magnesiowüstite are lower [*Duffy and Anderson*, 1989; *Yeganeh-Haeri et al.*, 1989]. In detail, the seismic properties of this assemblage will be affected by the rapid increase in temperature across *D*″ and by chemical reactions with the core [*Knittle and Jeanloz*, 1989*b*]. Such reactions will probably affect the Fe/Mg ratio of magnesiowüstite as well as its abundance relative to silica. Further, the extent and type of reaction will be strongly influenced by lateral temperature gradients and material transport caused by convective flow. Thus the chemistry of the oxide assemblage in *D*″ could be highly

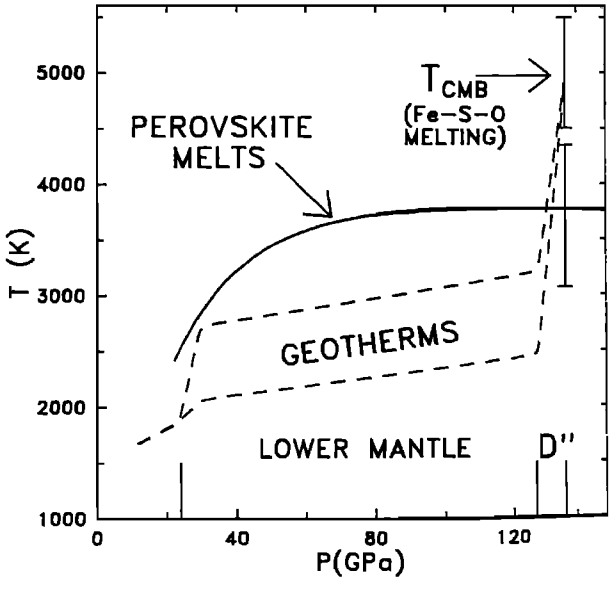

Fig. 16. Melting curve of perovskite predicted here (solid curve) compared with proposed geotherms (dashed curves) taken from *Jeanloz and Morris* [1986]. The lower and upper geotherms are for mantles which convect in one and two layers, respectively. The temperature point at the core-mantle boundary is constrained by the experimental study of melting in the Fe-S-O system by *Williams and Jeanloz* [1990].

variable, broadly consistent with the strong, lateral, seismic heterogeneity observed in this layer [*Young and Lay*, 1987].

As any discussion of the constitution of the D'' zone, ours is unavoidably somewhat speculative. Its relevance depends on the assumption that the melting curve of $MgSiO_3$ perovskite is indeed bounded by the hatched region in Figure 14, which in turn hinges on the accuracy of the theoretical equation of state of liquid perovskite. However, the accuracy of the diopside equation of state and the good agreement with the perovskite melting data suggest that, at least up to about 90 GPa, the liquid perovskite equation of state is accurate. There remains the possibility that the liquid stiffens rapidly above these pressures, perhaps because of a mechanism similar to that suggested by *Stolper and Ahrens* [1987]. As we have already argued, there is no solid evidence that such a mechanism operates in liquid silicates. Monte Carlo simulations show that bond breaking and reconnection, which result in significant network rearrangement, provide a very efficient means of stress relief and compressibility in liquid silica [*Stixrude and Bukowinski*, 1989]. The presence of network modifiers in liquid silicates should further enhance this process since they can encourage Si-O bond breaking. It is therefore far from obvious that the stiffening suggested by *Stolper and Ahrens* [1987], which results from a "kinking" of the network without bond breaking, actually takes place in liquid perovskite. Until shown otherwise by new data, it must be admitted that the calculated equation of state, and hence the melting curve, may be correct even in the D'' zone. We therefore present our speculations about D'' without apology and hope that they stimulate some interesting investigations and discussions.

Summary

The fundamental thermodynamic relation formalism is general and is applicable to all problems regarding the thermodynamics of the Earth's interior, including equations of state, phase equilibria, and melting. We have reviewed a particular, physically based form of the fundamental relation for solids (Debye thermal energy and Birch-Murnaghan finite-strain theory combined in the Mie-Grüneisen framework) which is known to provide an excellent description of solid-state thermodynamics. We found optimal fundamental relation parameters for four minerals of geophysical interest (diopside, enstatite, ilmenite, and perovskite) and found the fundamental relation to be in excellent agreement with data, including heat capacities, thermal expansion, and $MgSiO_3$ phase equilibria. By taking the high-temperature limit of the solid fundamental relation, we derived a fundamental relation for liquids and tested the accuracy of its equation of state. The liquid equation of state, which contains only four parameters, matched experimental data over a wide range of pressure and temperature for liquid alkali metals, water, and liquid diopside.

We combined liquid and solid fundamental relations to calculate the melting curves of diopside, enstatite, and perovskite, all of which were in good agreement with experiment. The melting curves all showed continuous reductions in the dT/dP melting slope with pressure, leading eventually to melting curve maxima and equilibrium liquid-crystal density inversion. This feature, which has not been exhibited by previous predictions, leads to a core-mantle boundary melting temperature of perovskite which is much lower than previous estimates, yet which is consistent with experimental data. If we accept recent estimates of outer core temperatures, our results imply that perovskite cannot be a constituent of D''. On the basis of a comparison of our results with seismic data we propose that D'' consists of (Mg, Fe)O magnesiowüstite and a silica phase, either stishovite or its recently discovered $CaCl_2$-type modification.

Acknowledgments. We thank D. Walker and an anonymous referee for their thorough reviews and R. Jeanloz, C. Lithgow, and D. Snyder for helpful comments on the manuscript. This work is supported by NSF grant EAR-8816819 and the Institute of Geophysics and Planetary Physics at the Lawrence Livermore National Laboratory.

References

Agee, C. B., and D. Walker, Static compression and olivine flotation in ultrabasic silicate liquid, *J. Geophys. Res.*, *93*, 3437–3449, 1988.

Agnon, A., and M. S. T. Bukowinski, Constraints on the thermal state of D'' from S wave velocities, *Eos Trans. AGU*, *69*, 494, 1988.

Anderson, D. L., and J. Bass, Transition region of the Earth's upper mantle, *Nature*, *320*, 321–328, 1986.

Anderson, O. L., The determination of the volume dependence of the Grüneisen parameter γ, *J. Geophys. Res.*, *79*, 1153–1155, 1974.

Anderson, O. L., R. Boehler, and Y. Sumino, Anharmonicity in the equation of state at high temperature for some geophysically important solids, in *High Pressure Research in Geophysics*, edited by S. Akimoto and M. H. Manghnani, pp. 273–283, Center for Academic Publishing, Tokyo, 1982.

Ashida, T., S. Kume, E. Ito, and A. Navrotsky, $MgSiO_3$ ilmenite: Heat capacity, thermal expansivity, and enthalpy of transformation, *Phys. Chem. Miner.*, *16*, 239–245, 1988.

Birch, F., Elasticity and constitution of the Earth's interior, *J. Geophys. Res.*, *57*, 227–286, 1952.

Birch, F., Finite strain isotherm and velocities for single-crystal and polycrystalline NaCl at high pressures and 300°K, *J. Geophys. Res.*, *83*, 1257–1268, 1978.

Birch, F., Equation of state and thermodynamic parameters of NaCl to 300 kbar in the high-temperature domain, *J. Geophys. Res.*, *91*, 4949–4954, 1986.

Boehler, R., Adiabats of quartz, coesite, olivine, and magnesium oxide to 50 kbar and 1000 K, and the adiabatic gradient in the Earth's mantle, *J. Geophys. Res.*, *87*, 5501–5506, 1982.

Boehler, R., and J. Ramakrishnan, Experimental results on the pressure dependence of the Grüneisen parameter: A review, *J. Geophys. Res.*, *85*, 6996–7002, 1980.

Boettcher, A. L., C. W. Burnham, K. E. Windom, and S. R. Bohlen, Liquids, glasses and the melting of silicates to high pressures, *J. Geol.*, *90*, 127–138, 1982.

Born, M., and K. Huang, *Dynamical Theory of Crystal Lattices*, 420 pp., Oxford University Press, New York, 1954.

Boschi, E., F. Mulargia, and M. Bonafede, The dependence of the melting temperatures of iron upon the choice of the interatomic potential, *Geophys. J. R. Astron. Soc.*, *58*, 201–208, 1979.

Bottinga, Y., On the isothermal compressibility of silicate liquids at high pressure, *Earth Planet. Sci. Lett.*, *74*, 350–360, 1985.

Bowen, N. L., *The Evolution of the Igneous Rocks*, 334 pp., Princeton University Press, Princeton, N. J., 1928.

Boyd, F. R., and J. L. England, Effect of pressure on the melting of diopside, $CaMgSi_2O_6$, and albite, $NaAlSi_3O_8$, in the range up to 50 kbar, *J. Geophys. Res.*, *68*, 311–323, 1963.

Boyd, F. R., J. L. England, and B. T. C. Davis, Effects of pressure on the melting and polymorphism of enstatite, $MgSiO_3$, *J. Geophys. Res.*, *69*, 2101–2109, 1964.

Bukowinski, M. S. T., and G. H. Wolf, Equation of state and possible critical phase transitions in $MgSiO_3$ perovskite at lower-mantle conditions, in *Structural and Magnetic Phase Transitions in Minerals*, edited by S. Ghose, J. M. D. Coey, and E. Salje, pp. 91–112, Springer-Verlag, New York, 1988.

Bukowinski, M. S. T., and G. H. Wolf, Thermodynamically consistent decompression: Implications for lower mantle composition, *J. Geophys. Res.*, *95*, 12,583–12,593, 1990.

Callen, H. B., *Thermodynamics and an Introduction to Thermostatistics*, 2nd ed., 493 pp., John Wiley, New York, 1985.

Chopelas, A., Thermal properties of forsterite at mantle pressures derived from vibrational spectroscopy, *Phys. Chem. Miner.*, *17*, 149–156, 1990.

Chopelas, A., and R. Boehler, Thermal expansion at very high pressure, systematics, and a case for a chemically homogeneous mantle, *Geophys. Res. Lett.*, *16*, 1347–1350, 1989.

Debye, P., Zur theorie der spezifischen Wärmen, *Ann. Phys.*, *39*, 789–839, 1912.

Depaolo, D. J., Nd isotopic studies: Some new perspectives on Earth structure and evolution, *Eos Trans. AGU*, *62*, 137–140, 1981.

Duffy, T. S., and D. L. Anderson, Seismic velocities in mantle minerals and the mineralogy of the upper mantle, *J. Geophys. Res.*, *94*, 1895–1912, 1989.

Dziewonski, A. M., and D. L. Anderson, Preliminary reference Earth model, *Phys. Earth Planet. Inter.*, *25*, 297–356, 1981.

Einstein, A., Die Plancksche theorie der Strahlung und die theorie der spezifischen Wärme, *Ann. Phys.*, *22*, 180–190, 1907.

Fei, Y., S. K. Saxena, and A. Navrotsky, Internally consistent data and equilibrium phase relations for compounds in the system MgO-SiO_2 at high pressure and high temperature, *J. Geophys. Res.*, *95*, 6915–6928, 1990.

Finger, L. W., and Y. Ohashi, The thermal expansion of diopside to 800°C and a refinement of the crystal structure at 700°C, *Am. Mineral.*, *61*, 303–310, 1976.

Flasar, F. M., and F. Birch, Energetics of core formation: A correction, *J. Geophys. Res.*, *78*, 6101–6103, 1973.

Frisillo, A. L., and G. R. Barsch, Measurement of single-crystal elastic constants of bronzite as a function of pressure and temperature, *J. Geophys. Res.*, *77*, 6360–6384, 1972.

Fyfe, W. S., The evolution of the Earth's crust: Modern plate tectonics to ancient hot spot tectonics?, *Chem. Geol.*, *23*, 89–114, 1978.

Grindley, T., and J. E. Lind, PVT properties of water and mercury, *J. Chem. Phys.*, *54*, 3983–3989, 1971.

Grüneisen, E., Theorie des festen zustandes einatomiger elemente, *Ann. Phys.*, *39*, 257–306, 1912.

Grüneisen, E., Zustand des festen Körpers, *Handb. Phys.*, *10*, 1–59, 1926.

Hanks, T. C., and D. L. Anderson, The early thermal history of the Earth, *Phys. Earth Planet. Inter.*, *2*, 19–29, 1969.

Hardy, R. J., Temperature and pressure dependence of intrinsic anharmonic and quantum corrections to the equation of state, *J. Geophys. Res.*, *85*, 7011–7015, 1980.

Harr, L., J. S. Gallagher, and G. S. Kell, *Steam Tables*, 320 pp. Hemisphere Publishing, New York, 1984.

Heinz, D. L., and R. Jeanloz, Measurement of the melting curve of $Mg_{0.9}Fe_{0.1}SiO_3$ at lower mantle conditions and its geophysical implications, *J. Geophys. Res.*, *92*, 11,437–11,444, 1987.

Herzberg, C. T., Chemical stratification in the silicate Earth, *Earth Planet. Sci. Lett.*, *67*, 249–260, 1984.

Hess, H. H., History of the ocean basins, in *Petrological Studies: A Volume in Honor of A. F. Buddington*, edited by A. E. J. Engel, H. L. James, and B. F. Leonard, pp. 599–620, Geological Society of America, Boulder, Colo., 1962.

Higgins, G., and G. C. Kennedy, The adiabatic gradient and the melting point gradient in the core of the Earth, *J. Geophys. Res.*, *76*, 1870–1878, 1971.

Horiuchi, H., M. Hirano, E. Ito, and Y. Matsui, $MgSiO_3$ (ilmenite-type): Single crystal X-ray diffraction study, *Am. Mineral.*, *67*, 788–793, 1982.

Isaak, D. G., O. L. Anderson, and T. Goto, Elasticity of single-crystal forsterite measured to 1700 K, *J. Geophys. Res.*, *94*, 5895–5906, 1989.

Ito, E., and E. Takahashi, Melting of peridotite at uppermost lower-mantle conditions, *Nature*, *328*, 514–517, 1987.

Ito, E., and E. Takahashi, Postspinel transformations in the system Mg_2SiO_4-Fe_2SiO_4 and some geophysical implications, *J. Geophys. Res.*, *94*, 10,637–10,646, 1989.

Jeanloz, R., Universal equation of state, *Phys. Rev. B*, *38*, 805–807, 1988.

Jeanloz, R., Shock wave equation of state and finite strain theory, *J. Geophys. Res.*, *94*, 5873–5886, 1989.

Jeanloz, R., and E. Knittle, Density and composition of the lower mantle, *Philos. Trans. R. Soc. London, Ser. A*, *328*, 377–389, 1989.

Jeanloz, R., and S. Morris, Temperature distribution in the crust and mantle, *Annu. Rev. Earth Planet. Sci.*, *14*, 377–415, 1986.

Kato, T., and M. Kumazawa, Garnet phase of $MgSiO_3$ filling the pyroxene-ilmenite gap at very high temperature, *Nature*, *316*, 803–805, 1985.

Kato, T., A. E. Ringwood, and T. Irifune, Constraints on element partition coefficients between $MgSiO_3$ perovskite and liquid determined by direct measurements, *Earth Planet. Sci. Lett.*, *90*, 65–68, 1989.

Kieffer, S. W., Thermodynamics of lattice vibrations of minerals, 3, Lattice dynamics and an approximation for minerals with application to simple substances and framework silicates, *Rev. Geophys.*, *17*, 35–59, 1979.

Knittle, E., and R. Jeanloz, Synthesis and equation of state of (Mg, Fe)SiO_3 perovskite to over 100 gigapascals, *Science*, *235*, 668–670, 1987.

Knittle, E., and R. Jeanloz, Melting curve of (Mg, Fe)SiO_3 perovskite to 96 GPa: Evidence for a structural transition in lower mantle melts, *Geophys. Res. Lett.*, *16*, 421–424, 1989*a*.

Knittle, E., and R. Jeanloz, Simulating the core-mantle boundary: An experimental study of high-pressure reactions between silicates and liquid iron, *Geophys. Res. Lett.*, *16*, 609–612, 1989*b*.

Knittle, E., R. Jeanloz, and G. L. Smith, Thermal expansion of silicate perovskite and stratification of the Earth's mantle, *Nature*, *319*, 214–216, 1986.

Knopoff, L., Equations of state at moderately high pressures, in *High Pressure Physics and Chemistry*, vol. 1, edited by R. S. Bradley, pp. 227–245, Academic, San Diego, Calif., 1963.

Knopoff, L., and J. N. Shapiro, Comments on the interrelationships between Grüneisen's parameter and shock and isothermal equations of state, *J. Geophys. Res.*, *74*, 1439–1450, 1969.

Kraut, E. A., and G. C. Kennedy, New melting law at high pressures, *Phys. Rev.*, *151*, 668–675, 1966.

Krupka, K. M., B. S. Hemingway, R. A. Robie, and D. M. Kerrick, High-temperature heat capacities and derived thermodynamic properties of anthophyllite, diopside, dolomite, enstatite, bronzite, talc, tremolite, and wollastonite, *Am. Mineral.*, *70*, 261–271, 1985.

Lange, R., and I. S. E. Carmichael, Densities of Na_2O-K_2O-CaO-MgO-FeO-Fe_2O_3-Al_2O_3-TiO_2-SiO_2 liquids: New measurements and derived partial molar properties, *Geochim. Cosmochim. Acta*, *51*, 2931–2946, 1987.

Lee, R. C., and L. R. Johnson, Extremal bounds on the seismic velocities in the Earth's mantle, *Geophys. J. R. Astron. Soc.*, *77*, 667–681, 1984.

Levien, L., and C. T. Prewitt, High-pressure structural study of diopside, *Am. Mineral.*, *66*, 315–323, 1981.

Levien, L., D. J. Weidner, and C. T. Prewitt, Elasticity of diopside, *Phys. Chem. Miner.*, *4*, 105–113, 1979.

Lindemann, F. A., Über die Berechnung molekulaner eigenfrequenzen, *Phys. Z.*, *11*, 609–612, 1910.

Liu, L., and W. A. Bassett, *Elements, Oxides and Silicates*, 250 pp., Oxford University Press, New York, 1986.

Lyzenga, G. A., T. J. Ahrens, W. J. Nellis, and A. C. Mitchell, The temperature of shock-compressed water, *J. Chem. Phys.*, *76*, 6282–6286, 1982.

Makarenko, I. N., A. M. Nikolaenko, and S. M. Stishov, Equation of state of liquid alkali metals: Sodium, potassium and caesium, in *Liquid Metals—1976*, edited by R. Evans and D. A. Greenwood, pp. 79–89, Institute of Physics, London, 1977.

Mie, G., Zur kinetischen theorie der einatomigen Körper, *Ann. Phys.*, *11*, 657–697, 1903.

Mulargia, F., and F. Quarreni, Validity of the Sutherland-Lindemann law and melting temperatures in the Earth's interior, *Geophys. J.*, *92*, 269–282, 1988.

Nisbet, E. G., and D. Walker Komatiites and the structure of the Archean mantle, *Earth Planet. Sci. Lett.*, *60*, 105–113, 1982.

Ohtani, E., Melting temperature distribution and fractionation in the lower mantle, *Phys. Earth Planet. Inter.*, *33*, 12–25, 1983.

Ohtani, E., Chemical stratification of the mantle formed by melting

in the early stage of the terrestrial evolution, *Tectonophysics*, *154*, 201–210, 1988.

Olinger, B., Compression studies of forsterite (Mg_2SiO_4) and enstatite ($MgSiO_3$), in *High Pressure Research*, edited by M. H. Manghnani and S. Akimoto, pp. 325–334, Academic, San Diego, Calif., 1977.

Plymate, T. G., and J. H. Stout, A five-parameter temperature-corrected Murnaghan equation for P-V-T surfaces, *J. Geophys. Res.*, *94*, 9477–9483, 1989.

Poirier, J. P., Lindemann law and the melting temperature of perovskites, *Phys. Earth Planet. Inter.*, *54*, 364–369, 1989.

Press, W. H., B. P. Flannery, S. A. Teukolsky, and W. T. Vetterling, *Numerical Recipes*, 818 pp., Cambridge University Press, New York, 1986.

Ralph, R. L., and S. Ghose, Enstatite, $Mg_2Si_2O_6$: Compressibility and crystal structure at 12 kbar, *Eos Trans. AGU*, *61*, 409, 1980.

Rigden, S. M., T. J. Ahrens, and E. M. Stolper, Densities of liquid silicates at high pressures, *Science*, *226*, 1071–1074, 1984.

Rigden, S. M., T. J. Ahrens, and E. M. Stolper, Shock compression of molten silicate: Results for a model basaltic composition, *J. Geophys. Res.*, *93*, 367–382, 1988.

Rigden, S. M., T. J. Ahrens, and E. M. Stolper, High-pressure equation of state of molten anorthite and diopside, *J. Geophys. Res.*, *94*, 9508–9522, 1989.

Rivers, M. L., and I. S. E. Carmichael, Ultrasonic studies of silicate melts, *J. Geophys. Res.*, *92*, 9247–9270, 1987.

Ross, M., Generalized Lindemann melting law, *Phys. Rev.*, *184*, 233–242, 1969.

Ross, N. L., and R. M. Hazen, Single crystal X-ray diffraction study of $MgSiO_3$ perovskite from 77 to 400 K, *Phys. Chem. Miner.*, *16*, 415–420, 1989.

Ruff, L., and D. L. Anderson, Core formation, evolution and convection: A geophysical model, *Phys. Earth Planet. Inter.*, *21*, 181–201, 1980.

Sasaki, S., and K. Nakazawa, Metal-silicate fractionation in the growing Earth: Energy source for the terrestrial magma ocean, *J. Geophys. Res.*, *91*, 9231–9238, 1986.

Sasaki, S., Y. Takéuchi, K. Fujino, and S. Akimoto, Electron-density distributions of three orthopyroxenes, $Mg_2Si_2O_6$, $Co_2Si_2O_6$, and $Fe_2Si_2O_6$, *Z. Kristallogr.*, *158*, 279–297, 1982.

Sawamoto, H., Phase diagram of $MgSiO_3$ at pressure up to 24 GPa and temperatures up to 2200°C: Phase stability and properties of tetragonal garnet, in *High Pressure Research in Mineral Physics*, *Geophys. Monogr. Ser.*, vol. 39, edited by M. H. Manghnani and Y. Syono, pp. 209–219, AGU, Washington, D. C., 1987.

Scarfe, C. M., and E. Takahashi, Melting of garnet peridotite to 13 GPa and the early history of the upper mantle, *Nature*, *322*, 354–356, 1986.

Schlosser, H., and J. Ferrante, Liquid alkali metals: Equation of state and reduced-pressure, bulk-modulus, sound-velocity, and specific-heat functions, *Phys. Rev. B*, *40*, 6405–6408, 1989.

Sclater, J. G., B. Parsons, and C. Jaupart, Oceans and continents: Similarities and differences in the mechanisms of heat loss, *J. Geophys. Res.*, *86*, 11,535–11,552, 1981.

Shapiro, J. N., and L. Knopoff, Reduction of shock-wave equations of state to isothermal equations of state, *J. Geophys. Res.*, *74*, 1435–1438, 1969.

Shaw, G. H., and D. A. Caldwell, Sound-wave velocities in liquid alkali metals studied at temperatures up to 150°C and pressures up to 0.7 GPa, *Phys. Rev. B*, *32*, 7937–7947, 1985.

Simon, F. E., The melting of iron at high pressures, *Nature*, *172*, 746–747, 1953.

Simozar, S., and L. A. Girifalco, Theoretical melting curve of caesium, *J. Phys. F*, *13*, 1145–1155, 1983.

Skinner, B. J., Thermal expansion, Handbook of Physical Constants, edited by S. P. Clark, *Mem. Geol. Soc. Am.*, *97*, 75–96, 1966.

Smith, A. H., and A. W. Lawson, The velocity of sound in water as a function of temperature and pressure, *J. Chem. Phys.*, *22*, 351–359, 1954.

Stacy, F. D., and R. D. Irvine, Theory of melting: Thermodynamic basis of Lindemann's law, *Aust. J. Phys.*, *30*, 631–640, 1977.

Stebbins, J. F., I. S. E. Carmichael, and L. K. Moret, Heat capacities and entropies of silicate liquids and glasses, *Contrib. Mineral. Petrol.*, *86*, 131–148, 1984.

Stevenson, D. J., Origin of the moon—The collision hypothesis, *Annu. Rev. Earth Planet. Sci.*, *15*, 271–315, 1987.

Stixrude, L., and M. S. T. Bukowinski, Simple covalent potential models of tetrahedral SiO_2: Applications to α-quartz and coesite at pressure, *Phys. Chem. Miner.*, *16*, 199–206, 1988.

Stixrude, L., and M. S. T. Bukowinski, Compression of tetrahedrally bonded SiO_2 liquid and silicate liquid-crystal density inversion, *Geophys. Res. Lett.*, *16*, 1403–1406, 1989.

Stolper, E. M., and T. J. Ahrens, On the nature of pressure-induced coordination changes in silicate melts and glasses, *Geophys. Res. Lett.*, *14*, 1231–1233, 1987.

Stolper, E., D. Walker, B. H. Hager, and J. F. Hays, Melt segregation from partially molten source regions: The importance of melt density and source region size, *J. Geophys. Res.*, *86*, 6261–6271, 1981.

Suzuki, I., Cell parameters and linear thermal expansion coefficients of orthopyroxenes, *J. Seismol. Soc. Jpn.*, *28*, 1–9, 1975.

Takahashi, E., Melting of a dry peridotite KLB-1 up to 14 GPa: Implications on the origin of peridotitic upper mantle, *J. Geophys. Res.*, *91*, 9367–9382, 1986.

Tsuchida, Y., and T. Yagi, A new post-stishovite high-pressure polymorph of silica, *Nature*, *340*, 217–220, 1989.

Uffen, R. J., A method of estimating the melting-point gradient in the Earth's mantle, *Eos Trans. AGU*, *33*, 893–896, 1952.

Vinet, P., J. Ferrante, J. R. Smith, and J. H. Rose, A universal equation of state for solids, *J. Phys. C*, *19*, L467–L473, 1986.

Vinet, P., J. R. Smith, J. Ferrante, and J. H. Rose, Temperature effects on the universal equation of state of solids, *Phys. Rev. B*, *35*, 1945–1953, 1987.

Wallace, D. C., *Thermodynamics of Crystals*, John Wiley, New York, 1972.

Watanabe, H., Thermochemical properties of synthetic high-pressure compounds relevant to the Earth's mantle, in *High Pressure Research in Geophysics*, edited by S. Akimoto and M. H. Maghnani, pp. 441–464, Center for Academic Publications, Tokyo, 1982.

Watt, J. P., and T. J. Ahrens, Shock wave equation of state of enstatite, *J. Geophys. Res.*, *91*, 7495–7503, 1986.

Webb, S. L., and I. Jackson, The anomalous pressure dependence of the elastic moduli for single-crystal orthopyroxene (abstract), *Eos Trans. AGU*, *66*, 371, 1985.

Weidner, D. J., and E. Ito, Elasticity of $MgSiO_3$ in the ilmenite phase, *Phys. Earth Planet. Inter.*, *40*, 65–70, 1985.

Weidner, D. J., H. Wang, and J. Ito, Elasticity of orthoenstatite, *Phys. Earth Planet. Inter.*, *17*, P7–P13, 1978.

Williams, D. W., and G. C. Kennedy, Melting curve of diopside to 50 kbar, *J. Geophys. Res.*, *74*, 4359–4366, 1969.

Williams, Q., and R. Jeanloz, Spectroscopic evidence for pressure-induced coordination changes in silicate glasses and melts, *Science*, *239*, 902–905, 1988.

Williams, Q., and R. Jeanloz, Melting relations in the iron-sulfur system at ultra-high pressures: Implications for the thermal state of the Earth, *J. Geophys. Res.*, in press, 1990.

Wolf, G. H., and R. Jeanloz, Lindemann melting law: Anharmonic correction and a test of its validity for minerals, *J. Geophys. Res.*, *89*, 7821–7835, 1984.

Xue, X., J. F. Stebbins, M. Kanzaki, and R. G. Tronnes, Silicon coordination and speciation changes in a silicate liquid at high pressures, *Science*, *245*, 962–964, 1989.

Yeganeh-Haeri, A., D. J. Weidner, and E. Ito, Single-crystal elastic moduli of magnesium metasilicate perovskite, in *Perovskite: A Structure of Great Interest to Geophysics and Materials Science*, *Geophys. Monogr. Ser.*, vol. 45, edited by A. Navrotsky and D. J. Weidner, pp. 13–25, AGU, Washington, D. C., 1989.

Young, C. J., and T. Lay, The core-mantle boundary, *Annu. Rev. Earth Planet. Sci.*, *15*, 25–46, 1987.

M. S. T. Bukowinski and L. Stixrude, Department of Geology and Geophysics, University of California, Berkeley, CA 94720.

(Received March 22, 1990;
revised July 9, 1990;
accepted July 30, 1990.)